Lung Cancer 134 (2019) 7–15

Contents lists available at ScienceDirect

Lung Cancer

journal homepage: www.elsevier.com/locate/lungcan

Paired genomic analysis of squamous cell carcinoma transformed from EGFR-mutated lung adenocarcinoma

Sehhoon Park[a,1], Joon Ho Shim[b,c,1], Boram Lee[b,c,1], Inju Cho[d], Woong-Yang Park[b,c], Youjin Kim[a], Se-Hoon Lee[a], Yoon La Choi[e], Joungho Han[e], Jin Seok Ahn[a], Myung-Ju Ahn[a], Keunchil Park[a], Jong-Mu Sun[a,*]

[a] Division of Hematology-Oncology, Department of Medicine, Samsung Medical Center, Sungkyunkwan University School of Medicine, Seoul, Republic of Korea
[b] Samsung Genome Institute, Samsung Medical Center, Sungkyunkwan University School of Medicine, Seoul, Republic of Korea
[c] Department of Health Science and Technology, Samsung Advanced Institute of Health Science and Technology, Sungkyunkwan University, Seoul, Republic of Korea
[d] Department of Hospital Pathology, Yeouido St. Mary's Hospital, The Catholic University, Seoul, Republic of Korea
[e] Department of Pathology and Translational Genomics, Samsung Medical Center, Sungkyunkwan University School of Medicine, Seoul, Republic of Korea

ARTICLE INFO

Keywords:
Adenocarcinoma
Carcinoma
Squamous cell
Non-small-cell lung
Receptor
Epidermal growth factor

ABSTRACT

Objectives: Adenocarcinoma (ADC) to squamous cell carcinoma (SCC) transformation (AST) is reported in epidermal growth factor receptor (EGFR)-mutated non–small cell lung cancer after tyrosine kinase inhibitor (TKI) failure. However, little is known about the underlying genomic changes during the AST process.
Materials and methods: We retrospectively reviewed our tissue database collected after first- or second- generation EGFR TKI resistance (n = 263) and identified 3 cases of AST. The additional case was acquired from the osimertinib resistance sample. Deep target sequencing (381 genes) using paired samples from 4 patients with AST after *EGFR* TKI treatment was performed. The histology of each sample was confirmed by TTF-1 and p63 immunohistochemistry. The patients received first- or second-generation *EGFR* TKI as an initial treatment.
Results: Overall incidence of AST was 1.1% (3/263). Transformed SCC acquired genomic alterations related to the PI3K/AKT/mTOR pathway, in addition to the initial *EGFR* mutation. In a representative case, two separate sub-clones, with a *PTEN* nonsense mutation and *EGFR* p.T790 M mutation, were observed without histologic transformation at the time of gefitinib resistance. After subsequent treatment with osimertinib, SCC transformation was observed with the disappearance of the *EGFR* p.T790 M mutation and acquired copy number loss in *PTEN*. Adopting the sub-clonal fraction model elucidates the sub-clonal evolution process of the *PTEN* mutant sub-clone toward AST under the background of *EGFR* mutation. The rest of the transformed samples also had acquired genomic alterations in *PTEN, LKB1, PIK3CA,* or *RICTOR*, which are related to the PI3K/AKT/mTOR pathway.
Conclusions: Paired genomic analysis from our sample provides early clinical evidence of the ADC to SCC lineage transition that might be provoked by an alteration in the PI3K/AKT/mTOR pathway during *EGFR* TKI treatment. This finding could potentially broaden the known spectrum of *EGFR* TKI resistance mechanisms.

1. Introduction

The standard care for lung adenocarcinoma (ADC) harboring an activating epidermal growth factor receptor (EGFR) mutation is treatment with *EGFR* tyrosine kinase inhibitor (TKI) [1,2]. Despite the promising efficacy of the initial therapy, nearly 14% of patients experience treatment resistance through histologic transformation, and the exact mechanism of that change remains unknown [3–5]. Recently, several cases of ADC to squamous cell lung cancer (SCC) transformation (AST) in *EGFR*-mutated non–small cell lung cancer (NSCLC) have been reported [6–11]. Given the previous understanding that ADC and SCC arise from distinct cells origins, AST was generally considered to indicate that pre-existing SCC gains dominance after *EGFR* TKI selection pressure [12,13].

However, some evidence suggests that AST is a consequence of tumor evolution. For example, a transformed SCC sample maintained

* Corresponding author at: Division of Hematology-Oncology, Department of Medicine, Samsung Medical Center, Sungkyunkwan University School of Medicine, 81 Irwon-ro, Gangnam-gu, Seoul 06351, Republic of Korea.
E-mail address: jongmu.sun@skku.edu (J.-M. Sun).
[1] These authors contributed equally to this study as co-first authors.

https://doi.org/10.1016/j.lungcan.2019.05.024
Received 5 March 2019; Received in revised form 21 May 2019; Accepted 23 May 2019

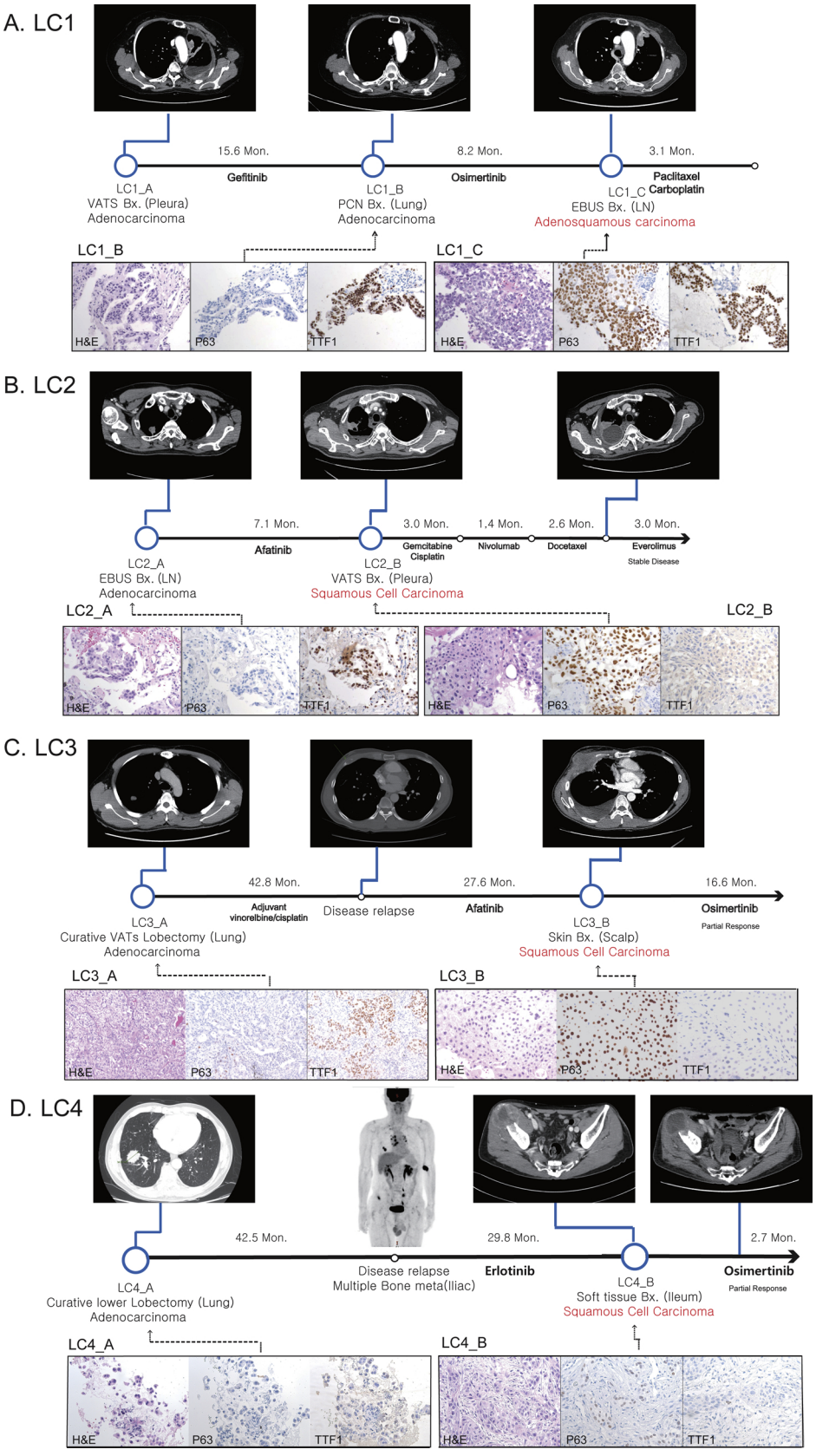

Fig. 1. Clinical history of the LC1, LC2, LC3, and LC4 patients. The blue circles indicate the time points of tumor biopsies. Samples were stained with hematoxylin and eosin, p63, and TTF-1. (*A*) The LC1 patient had three biopsies: at diagnosis (Dx), the first relapse to gefitinib, and second relapse to osimertinib. (*B*) The LC2 patient had biopsies at Dx and post-afatinib failure. This patient is currently under treatment with everolimus. (*C*) The LC3 patient had biopsies at Dx and post-afatinib failure. This patient is currently under treatment with osimertinib. (*D*) The LC4 patient had biopsies at Dx and post-erlotinib failure. This patient is currently under treatment with osimertinib. (For interpretation of the references to colour in this figure legend, the reader is referred to the web version of this article.)
Abbreviations: VATS, video-assisted thoracoscopic surgery; PCN, percutaneous needle; Bx, biopsy; EBUS, endobronchial ultrasound; LN, lymph node; IHC, immunohistochemistry; H&E, Hematoxylin and eosin.

its initial *EGFR* mutations, even after complete histology changes and with no remaining ADC component [14–16]. Nonetheless, little is known about the underlying genetic mechanisms of histologic transformation. A case report described target sequencing with transformed SCC and found the acquisition of a missense mutation in *PIK3CA*, as well as an *EGFR* mutation (L858R), but it failed to show whether the *PIK3CA* mutation was newly acquired during AST because baseline samples were unavailable for comparison [7,17].

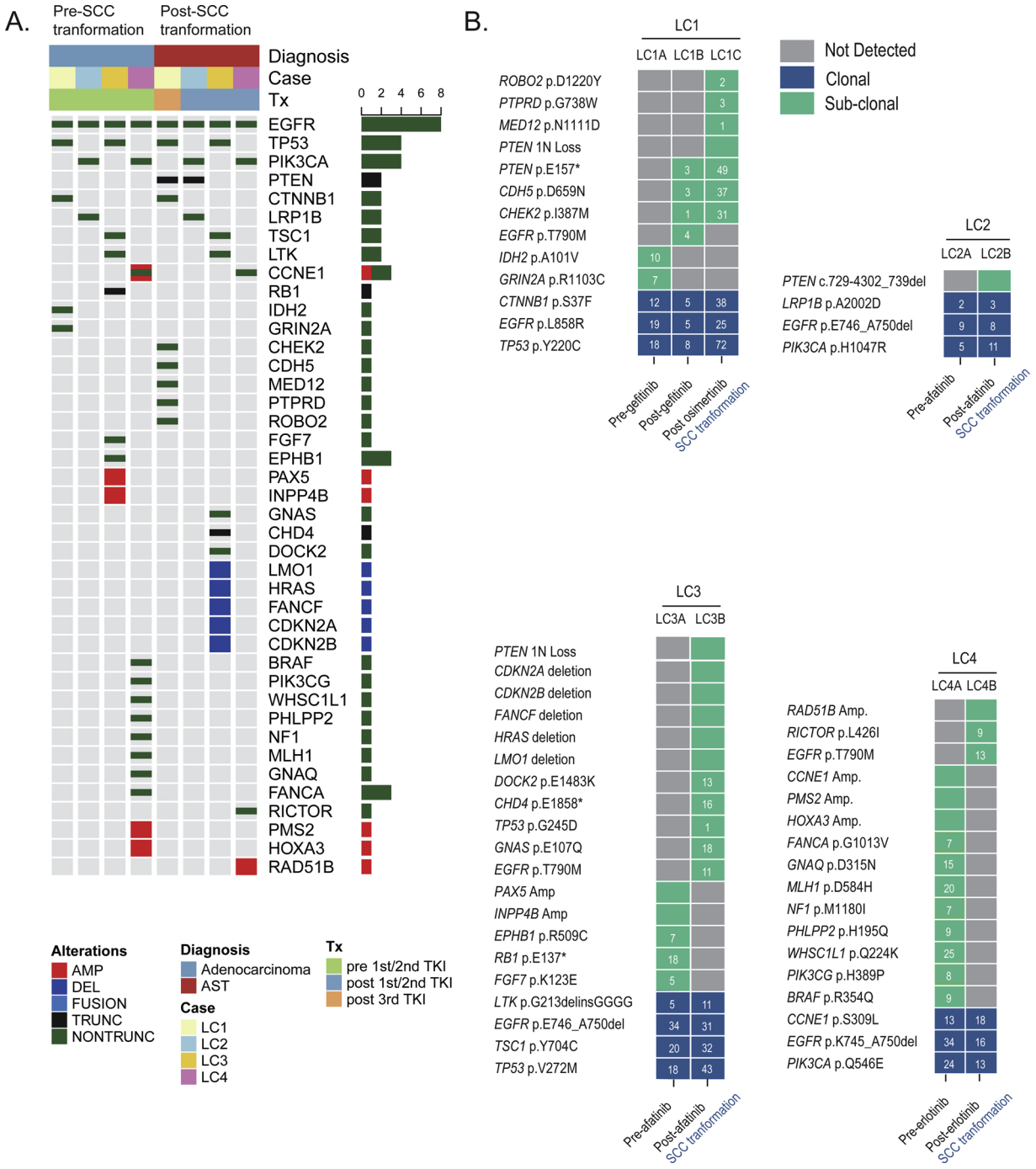

Fig. 2. (A) Overall mutational landscape of study samples, (B) Longitudinal analysis of treatment-induced genomic profile evolution. Heatmap is illustrating genomic profile evolution under the pressure of targeted therapy. Mutation is classified as sub-clonal if mutation is disappeared or newly appeared during the treatment. Number in the box is indicating variant allele fraction of each mutation. (For interpretation of the references to colour in this figure legend, the reader is referred to the web version of this article.)
Abbreviation: SCC, squamous cell carcinoma.

Other evidence comes from a preclinical mouse model that simulated AST by *KRAS* mutation and the suppression of *LKB1*. In this mouse model, depletion of *LKB1,* which is known to suppress tumors by negatively regulating mTOR, was observed as a pivotal component in the histologic transformation of AST; the proportion of the SCC component increased after the initial presentation of ADC in normal lung tissue [18,19]. In a similar way, another mouse model with both *LKB1* and *PTEN* deletion led to pure SCC, without the presentation of an ADC component during the transformation [20].

Based on those observations, we hypothesized that ADC and SCC could share a common lineage and acquire different phenotypes through a lineage transition provoked by the accumulation of genomic alterations, especially in the PI3K/AKT/mTOR pathway [21]. To elucidate the underlying genomic changes that occur during AST, we collected pre- and post-samples from transformed SCC cases and conducted a paired comparison of the mutation profiles using deep target sequencing.

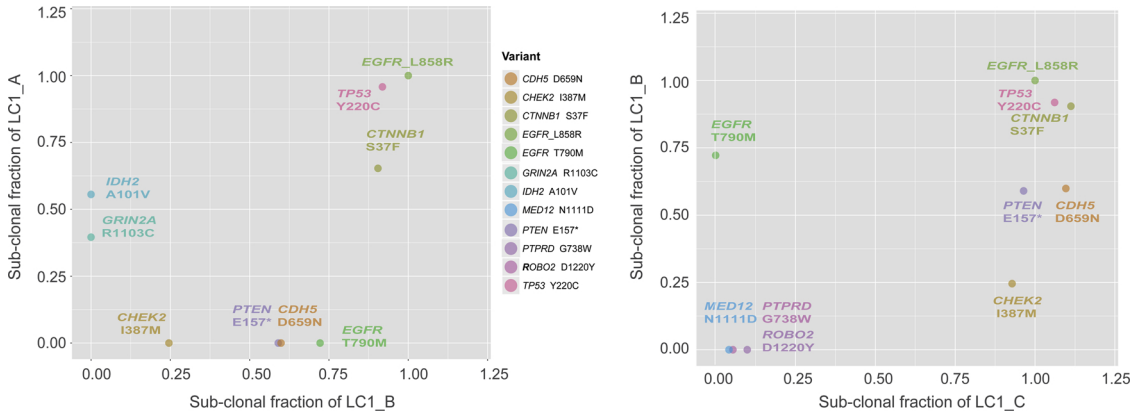

Fig. 3. Two-dimensional plotting of sub-clonal fraction in the LC1 patient. The distribution of sub-clonal fraction was compared in longitudinal tumor samples acquired at initial presentation (LC1_A), at the time of first-line treatment failure (LC1_B), and at repeat biopsy, which demonstrated adenosquamous cell carcinoma histology (LC1_C). The x-axis of each graph indicates newly emerged sub-clones, and the y-axis indicates eradicated sub-clones. Six clusters of somatic base substitutions were inferred by the distribution of the sub-clonal fraction and used for phylogeny analysis.

2. Material and methods

2.1. Patients and samples

We retrospectively reviewed our database who treated with either first- or second- generation EGFR TKI as a first-line treatment between January 2014 and December 2016 at Samsung Medical Center (n = 524). Among the patients who have conducted the second biopsy after the disease progression (n = 263), we identified three NSCLC patients initially diagnosed as having ADC with an activating *EGFR* mutation that acquired an SCC histology after *EGFR* TKI treatment. Additional one case was identified from the sample acquired after the osimertinib treatment.

Formalin-fixed, paraffin embedded (FFPE) tissues or fresh frozen tissues from either the primary tumor or metastatic sites were used for the histologic and genomic analyses. This study was approved by the institutional review board of Samsung Medical Center (IRB approval no. SMC-2016-03-094), and informed consent was obtained from the patients.

2.2. Isolation of genomic DNA

All tumor specimens were reviewed by pathologists to determine the percent of viable tumor and adequacy for sequencing. Genomic DNA was extracted from FFPE tissue using a Qiagen DNA FFPE tissue kit, and genomic DNA was extracted from fresh tissue using a QIAamp DNA mini kit (Qiagen, Valencia, CA, USA). Genomic DNA concentration and purity were measured with a Nanodrop 8000 UV–vis spectrometer (Thermo Scientific Inc., DE, USA) and a Qubit 2.0 fluorometer (Life Technologies Inc., Grand Island, NY, USA). To estimate DNA degradation, DNA median size and ΔCt values were measured with a 2200 TapeStation Instrument (Agilent Technologies, Santa Clara, CA, USA) and real-time PCR (Agilent Technologies), respectively.

2.3. Sequencing using a cancer panel (CancerSCAN™)

Genomic DNA (250 ng) from each tissue was sheared in a Covaris S220 ultrasonicator (Covaris, Woburn MA, USA) and used to construct a library with CancerSCAN™ probes and a SureSelect XT reagent kit (HSQ, Agilent Technologies), following the manufacturer's protocol. This panel is designed to enrich exons of 381 genes curated from the literature (Table A1 in Supplementary material) [22,23]. After the enriched exome libraries were multiplexed, they were sequenced using the 100-bp paired-end mode of the TruSeq Rapid PE cluster kit and TruSeq Rapid SBS kit on the Illumina HiSeq 2500 sequencing platform (Illumina Inc., San Diego, CA, USA). The DNA sequence data were aligned to the human genome reference (hg19) using the MEM algorithm in BWA 0.7.5 [24]. Duplicated read removal was performed using Picard v.193 and SAMTOOLS v0.1.18 (samtools.sourceforge.net). Local alignment was optimized using the Genome Analysis Toolkit (GATK) v3.1-1 (https://software.broadinstitute.org/gatk/). We also used BaseRecalibrator from GATK for base recalibration with known single nucleotide polymorphisms (SNPs) and insertions/deletions (indels) from Mills, dbSNP138, 1000 G gold standard, 1000 G phase1, and Omni 2.5. Quality control data are described in Table A2 in Supplementary material.

2.4. Variant detection

Variant calling was done only in regions targeted in CancerSCAN™. We detected single-nucleotide variants (SNVs) using two tools: MuTect v1.14 and LoFreq v0.61 [25,26]. Then, we filtered out falsely detected variants from abnormally aligned, strand-biased, and clustered reads using in-house developed scripts. ANNOVAR was used to annotate the detected variants. Indels less than 30 bp were detected by Pindel and annotated by ANNOVAR [27]. To filter out germline variants, we applied two algorithms: i) Suspect germline variants were filtered out based on a minor allele frequency (MAF) greater than or equal to the normal population in the 1000 Genomes Project, ExAC, Korean Reference Genome Database, and Korean Variant Archive [28]; ii) When the fraction of the clone with the variant was larger than the tumor purity, we considered that variant as a germline. Tumor purity was inferred from the B-allele fractions of the copy-neutral, gain, and loss regions. Deletions of more than 30 bp were detected using an in-house structure variation caller. The copy number of the target genes was detected using an in-house copy number caller [22]. Assuming that the estimated tumor purity can vary as much as 10%, we called 1 copy deletion if the adjusted copy number is less than 0.87 and there is loss of heterozygosity (LOH) in the nearby region.

2.5. Adjusted method for evaluating clonal evolution

We defined the cancer cell fraction (CCF) as the fraction of a clone with a certain SNV in the tumor sample, in a similar manner reported from the previous report [29]. The number of chromosomal copies at each SNV in the tumor was identified as the adjusted coverage relative to the copy number–neutral regions and inferred by selecting the closest positive integer value. Once the copy-neutral, gain, and loss regions have been delineated, the following formula can be used to infer the CCF of each tumor sub-clone having specific variant:

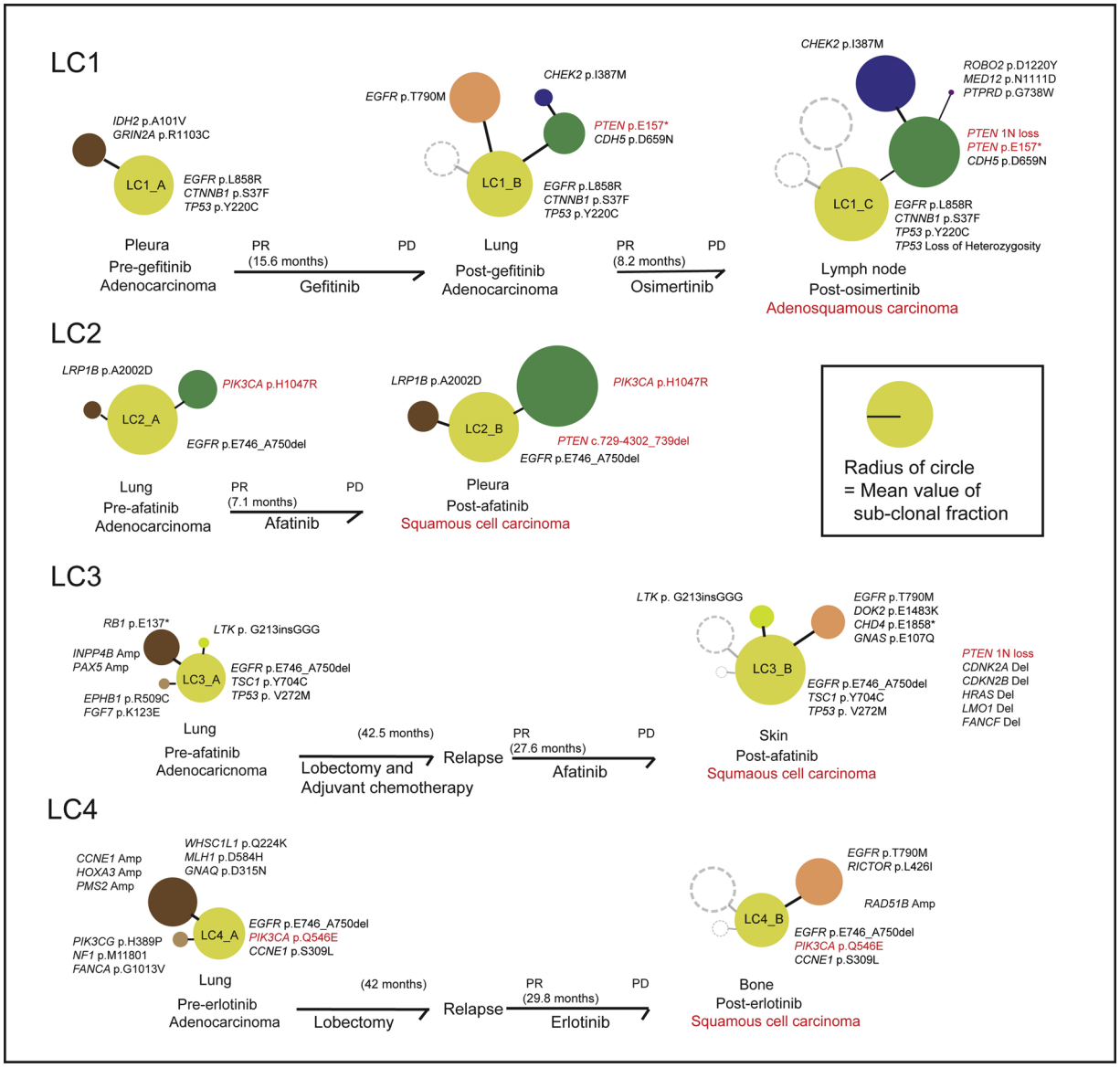

Fig. 4. Pictorial representation of the clonal evolutionary history of AST and phylogeny analysis of serially acquired tumor samples. Each circle indicates the major sub-clones of the tumors. Genetically defined sub-clones were manually clustered based on a two-dimensional comparison of the sub-clonal fractions in Fig. 3 and Appendix Fig. 5 in Supplementary material. The radius of each circle is proportional to the mean value of the sub-clonal fraction. The clinical history is summarized beneath the black arrows. Genetic alterations in the PI3K/AKT/mTOR pathway (*PIK3CA* and *PTEN*) are marked in red. (For interpretation of the references to colour in this figure legend, the reader is referred to the web version of this article.)
Abbreviations: AST, adenocarcinoma to squamous cell carcinoma transformation; Amp, amplification; Del, deletion.

$$VAF_v = \frac{CCF_v \times X_v}{2 \times (1 - CCF_v) + CN_v \times CCF_v}$$

Where CN_v is the copy number of a gene where a variant v is present, which is equal to the sum of the numbers of the reference allele and the alternative allele, X_v is the numbers of the alternative allele of the v, and CCF_v is the cancer cell fraction of the sub-clone having the v. Loss of heterozygosity (LOH) in nearby region was considered in deciding each X value. We assumed that each *EGFR* driver mutations (e.g., *EGFR* p.L858R or exon 19 deletion)are fully clonal in *EGFR*-mutant NSCLC based on the previous reports indicating that *EGFR* mutations are dominant truncal drivers in *EGFR*-mutant ADC [30–32]. At the same time, we assumed that sub-clonal fraction could be calculated by the CCF of individual variant divided by the CCF of dominant truncal drivers. When deciding X_{EGFR_driver} value, CCF_{EGFR_driver} was compared with the highest CCF value of the sample to meet the assumption that the *EGFR* driver mutation is a truncal mutation. A sub-clonal fraction is calculated based below equation using CCF_{EGFR_driver} and CCF_v.

$$\text{Sub-clonal fraction} = \frac{CCFv}{CCF_{EGFR\_driver}}$$

If sub-clonal fraction estimates are greater than 1, we assume that these variants are fully clonal within the tumor.

2.6. Pathology and immunohistochemistry

FFPE samples were used for hematoxylin and eosin staining and immunohistochemical (IHC) study. IHC staining of p63 (BIOCARE, CM163C, mouse monoclonal, 1:200 dilution) and TTF1 (DAKO, M3575, mouse monoclonal, 1:100 dilution) was performed. FFPE tissue sections (4-μm thick) were stained automatically (BONDMAX) using standard methods. All pathology slides were examined by three pathologists with expertise in lung cancer pathology (B.R.L., Y.L.C., and I.J.C.).

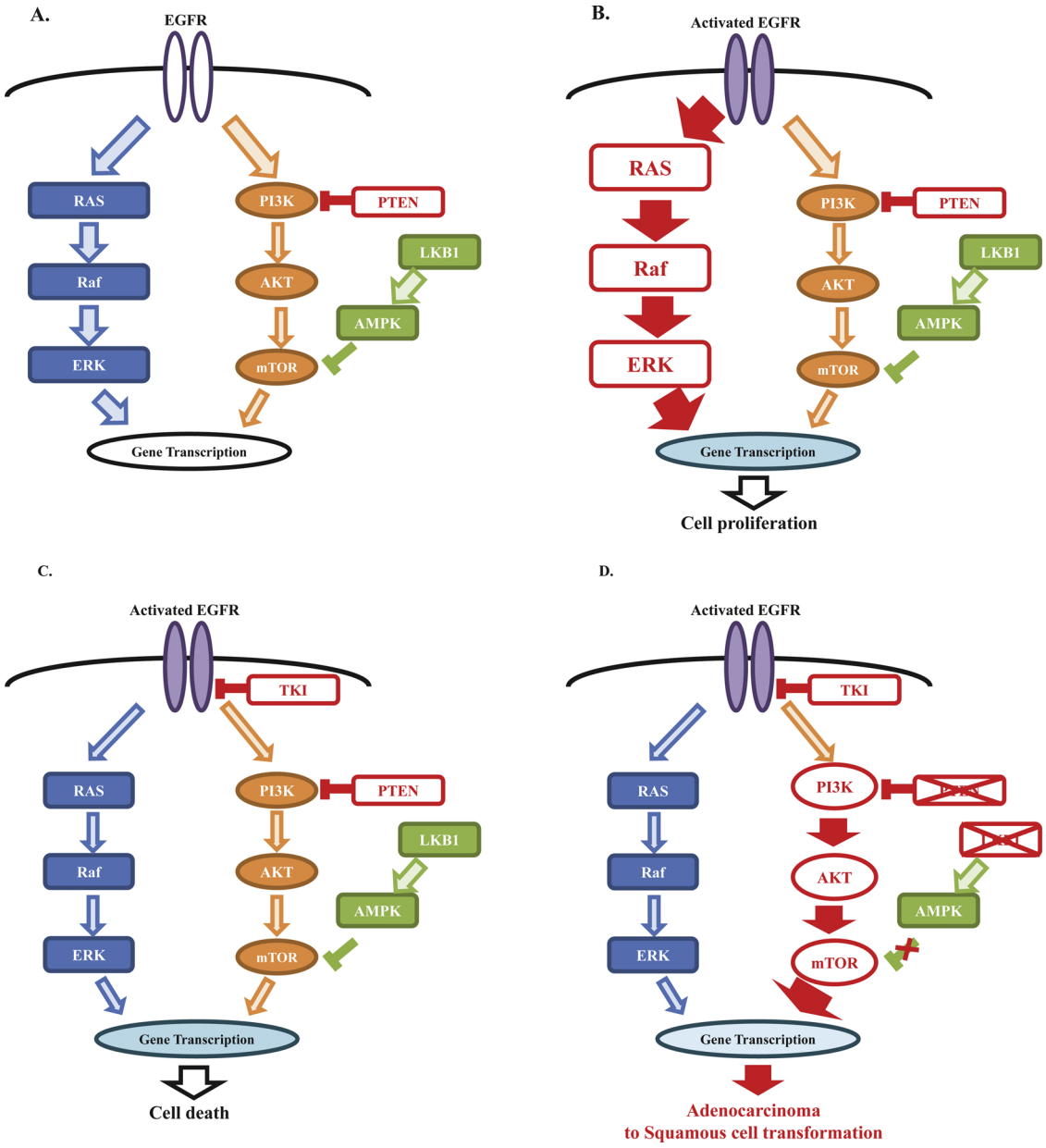

Fig. 5. Hypothesis based on EGFR and the PI3K/AKT/mTOR pathway. (A) In normal tissue, both *EGFR* and the PI3K/AKT/mTOR pathway are activated under proper regulation by *PTEN* and *LKB1*. (B) In a cancer cell with an activating *EGFR* mutation, oncogene addiction occurs by activating the *EGFR* signal pathway. (C) *EGFR* TKI suppresses both the Ras/Raf/MAPK and PI3K/AKT/mTOR signal pathways, which leads to cell death. (D) In addition to *EGFR* TKI, *PTEN* and *LKB1* loss lead to uncontrolled activation of the PI3K/AKT/mTOR pathway, which can be hypothesized as a favorable circumstance for adenocarcinoma to squamous cell carcinoma transformation.

3. Results

3.1. Clinical characterization of patients with AST

The overall incidence of AST after treatment of either first- or second generation TKI was 1.1% (3 out of 263). The LC1 patient (65 years, female) with an initial *EGFR* L858R mutation (LC1_A) was treated with gefitinib. However, subclone with acquired resistance to the gefitinib through an *EGFR* p.T790 M mutation without histologic change was observed (LC1_B). After subsequent second-line osimertinib treatment for 8.2 months, adenosquamous histology with the disappearance of the *EGFR* p.T790 M mutation was observed in a LC1_C (Fig. 1a). The LC2 patient (56 years, male), with an *EGFR* exon 19 deletion, was treated with afatinib for 7.1 months. Squamous histology with *EGFR* exon 19 deletion was observed in a post-afatinib biopsy. After 3 additional therapies, the LC2 patient is currently under treatment with everolimus (mTOR inhibitor) for 3 months, and his pleuritic pain has decreased with the radiological improvement of the right middle lobe atelectasis (Fig. 1b and Fig. A1 in Supplementary material). The LC3 patient (40 years, male), with *EGFR* exon 19 deletion, had a tumor recurrence after curative surgery, relapsing after a 42.8-month disease-free period. After treatment with afatinib for 27.6 months, squamous histology with an initial *EGFR* exon 19 deletion and new *EGFR* p.T790 M mutation was observed. A partial response was acquired following osimertinib treatment (Fig. 1c). The LC4 patient (67 years, male), with an *EGFR* exon 19 deletion, was treated with erlotinib for 29.8 months as a first-line treatment. The resistant sample showed squamous histology with an initial *EGFR* exon 19 deletion and new *EGFR* p.T790 M mutation and showed a partial response to osimertinib treatment (Fig. 1d). Notably, all SCCs after TKI treatment were positive

for the p63 stain and maintained the initial *EGFR* mutation observed in the ADC histology. Detailed treatment histories are described in Table A3 in Supplementary material.

3.2. Transformed SCC acquires genomic alterations related to the PI3K/AKT/mTOR pathway

All of the transformed SCC samples had an acquired genomic alteration related to the PI3K/AKT/mTOR pathway. The LC1_B post-gefitinib sample (from the LC1 patient) had new non-synonymous mutations in *CDH5* p.D659N, *CHEK2* p.I387M, *EGFR* p.T790M, and *PTEN* p.E157* with an ADC histology. Among the alterations, the one in *PTEN* p.E157* was a stop gain mutation with a VAF of 3.2%. The LC1_C sample after osimertinib had a loss of heterozygosity in *PTEN*. The VAF of PTEN p.E157* increased to 48.9%, and copy number loss (1n) was observed in *PTEN* in the LC1_C sample, which indicates a complete loss of *PTEN* function (Fig. A2 in Supplementary material). The LC2_B sample had an acquired splice site deletion in *PTEN* c.729-4302_739del, in addition to a clonal *PIK3CA* mutation. In the LC3 patient, *PTEN* loss (1n) was also observed in the post-afatinib sample. The LC4 samples had a clonal mutation in *PIK3CA* p.Q54B and *RICTOR* p.L426I, a rapamycin-insensitive companion of mTOR that is an upstream kinase in the AKT pathway and related to cell proliferation and survival [29]. *RICTOR* p.L426I had a VAF of 8.8% in the LC4_B sample (Fig. 2, Table A4 in Supplementary material).

3.3. Alteration in mTOR function by copy number variation in LKB1

Based on a preclinical model suggesting that *LKB1* loss could be an important determinant of lung squamous tumorigenesis [19], we used an additional tool (PureCN [30]) to measure copy number loss and loss of heterozygosity (LOH) of *LKB1* gene. LC1_A, LC1_C, LC2_B, LC3_B, LC4_A, and LC4_B samples showed LOH (Fig. A3 in Supplementary material). Acquired copy number deletion in both alleles *LKB1* gene was found in the LC2_B sample (Fig. A4 in Supplementary material). In short, there was acquired 19p13.3 copy number deletion in LC2_B and acquired LOH in the *LKB1* gene region in LC2_B and LC3_B. LC1 and LC4 samples had LOH from the initial presentation.

3.4. PTEN loss during clonal evolution of AST

To elucidate the clonal evolution process during AST, we adopted the sub-clonal fraction model. Based on the assumption that all tumor-cell evolution occurs from a common ancestor clone that harbors the *EGFR* mutation, we plotted sub-clones based on their sub-clonal fraction value (Fig. 3, Fig. A5 in Supplementary material). As a representative case, we made an initial comparison between the LC1_A and LC1_B samples. Newly appearing sub-clones were plotted on the x-axis marked with the *EGFR* p.T790 M and *PTEN* p.E157* mutations. As shown in Fig. 3, a clone with the *PTEN* mutation showed a stepwise increase in its sub-clonal fraction. In contrast to the low VAF value (3.2%) of *PTEN* in the LC1_B sample, the sub-clonal fraction was close to 59.0%, which indicates *PTEN* heterozygosity in the *EGFR*-mutated tumor cells. The next analysis was conducted by directly comparing the LC1_B and LC1_C samples. The sub-clonal fraction of *PTEN* p.E157* increased to 96.4% as a consequence of the LOH, resulting in a copy number loss of the wild type *PTEN* (Fig. A2 in Supplementary material). Applying this method to other samples showed an increase in the *PIK3CA* mutated sub-clone (sub-clonal fraction change from 56.0% to > 99.9%) in the LC2 samples. In the LC4 samples, the acquired *RICTOR*-mutated sub-clone (sub-clonal fraction change from 0% to 55.1%) developed under the background of *PIK3CA* p.Q546E mutation in the transformed SCC (Table A4 in Supplementary material). This approach had limitations for visualizing genes with copy number variations without an underlying mutation, as shown in the case of the *PTEN* loss in the LC3_B sample.

3.5. The clinical implications of genomic alteration in transformed SCC

Using the sub-clonal fraction method, we created an arbitrary clustering approach using the distance from the CCF plot to simplify the evolutional process of AST (Fig. 4). This approach visualizes the process of sub-clonal evolution and provides clear evidence for the dominant mutation. Adopting this analysis to clinical practice, we considered an exploratory treatment approach to the LC2 patient in a salvage setting. The LC2 patient received four different treatments, including a cytotoxic drug, an immune checkpoint inhibitor, and *EGFR* TKI. With no treatment option available as standard care and considering the dominant mutation in *PI3KCA*, *PTEN* deletion, and loss of *LKB1* functions in LC2_B, we treated the LC2 patient with an mTOR inhibitor as a fifth-line treatment. Surprisingly, the patient demonstrated stable disease for 3.0 months with both radiologic and symptomatic improvement. The LC3_B and LC4_B samples had a relatively high (43.9% and 79.0%) sub-clonal fraction for EGFR p.T790 M. Despite a report that SCC with an activating *EGFR* mutation responds more poorly to *EGFR* TKI than ADC [31], both the LC3 and LC4 patients showed an ongoing partial response to osimertinib.

4. Discussion

The result of this study involves the paired genomic outcomes between pre- and post- sample from AST. This approach provides meaningful clues to the several unmet questions regarding the histologic transformation.

Our findings support the idea that AST could be an outcome of evolution. Looking into the representative result from the LC1 patient, we found a fascinating evolution in the *PTEN* tumor suppressor gene. The LC1_B sample showed *EGFR* p.T790 M (VAF 3.8%) and *PTEN* p.E157* (VAF 3.0%, copy number [CN] 1.82) nonsense mutations after treatment with gefitinib. At that time point, *EGFR* p.T790 M and *PTEN* p.E157* were clustered separately, as shown in Fig. 3, indicating the co-presentation of two separate sub-clones that shared the *EGFR* mutation in the LC1_A sample as an ancestor clone (Fig. A2 in Supplementary material). After 8.3 months of following osimertinib treatment, increased *PTEN* p.E157* fraction (VAF 48.9%) and *PTEN* CN loss (1.28) were observed, which consequences the complete loss of *PTEN* tumor suppressor function in all *EGFR*-mutated tumor cells. At the same time, the sub-clonal fraction increased to 96.4%. This explains the clonal selection process in our sample: *PTEN* p.E157* sub-clones dominated after osimertinib treatment (Fig. 4).

Our result also supports the idea that AST occurs when ADC acquires certain mutations, such as active genomic alterations in the PI3K/AKT/mTOR pathway. From the preclinical study, we found major evidence related to the activation of the PI3K/AKT/mTOR pathway, which could be a core component of the histologic transformation from ADC to SCC. In a preclinical AST model conducted with an *LKB1*-deficient and *KRAS* G12D-driven ADC mouse model [18], PI3K/AKT/mTOR pathway was activated through the loss of the negative regulation of mTORC1 [32]. The importance of the activated PI3K/AKT/mTOR pathway in the development of SCC tumorigenesis was also researched using an in vivo mouse model without a *KRAS* mutation [20]. Unlike the *KRAS*-mutated *LKB1*-deficient mouse model, in which most mice initially developed an ADC histology, mice with biallelic *PTEN*- and *LKB1*-deficiency developed pure SCC [20]. Among our samples, the LC2_B sample predominantly showed acquired genomic alterations in the PI3K/AKT/mTOR pathway. The LC2_B sample had an acquired deletion mutation, *PTEN* c.729-4302_739del, under the background of *PIK3CA* p.H1047R, which is identical to a mutation in a previously reported AST case [7]. Notice that the sub-clonal fraction of *PIK3CA* p.H1047R in the LC2_B SCC sample increased from 56.0% to > 99.9%, indicating that all the *EGFR* TKI–resistant *EGFR* exon-19-deleted sub-clones possessed the mutation in *PIK3CA*. In addition to the *PIK3CA* mutation and *PTEN* loss, complete deletion (0 N) of the locus containing

LKB1, which could activate mTOR, was observed in the transformed SCC sample (LC2_B).

Nonetheless, questions remain. For example, why do *PTEN*-mutated ADC cells not always transform into SCC? Given that little is known about the discovery rate of co-developed activating *EGFR* mutations and *PTEN* deletions in the same tumor (Fig. A6 in Supplementary material), we used our observations to link our finding with activated *EGFR* pathway. EGFR promotes cellular proliferation through both the Ras/Raf/mitogen-activated protein kinase (MAPK) pathway and the PI3K/AKT/mTOR pathway (Fig. 5a) [33]. With an activating *EGFR* mutation and intact *PTEN* function, cellular proliferation could rely mainly on the Ras/Raf/MAPK pathway (Fig. 5b). However, when *EGFR* TKI is applied to those patients, both the Ras/Raf/ERK and PI3K/AKT/mTOR pathways are suppressed, leading to cell death (Fig. 5c) [18]. Given the preclinical evidence and what our samples show, when *EGFR* pathway is suppression with TKI and *PTEN* or *LKB1* are lost, cellular proliferation dependency on the PI3K/AKT/mTOR pathway might increase, which could lead to AST in tumors with an activating EGFR mutation (Fig. 5d).

In this study, it was difficult to find substantial evidence linking AST with *EGFR* TKI failure. Perhaps, AST cases that follow the failure of *EGFR* TKI treatment without a known resistance mechanism support the possibility of AST as a novel mechanism of treatment failure [6–9,21]. However, some reports have proposed that activating the PI3K/AKT/mTOR pathway through *PTEN* loss without histologic changes could also contribute to *EGFR* TKI resistance [34]. Moreover, the presence of the *EGFR* p.T790 M mutation, which is a well-known resistance mechanism for first- and second-generation EGFR TKI [5], in the LC3 and LC4 patients weakens the relationship between TKI resistance and AST. Altogether, careful interpretation needs to be made in drawing out the connections between AST and *EGFR* TKI resistance.

Although we proposed an additional dataset and hypothesis for AST based on somatic mutations and copy number alterations, our ability to validate the pathway activity is limited by the unavailability of gene expression data. At the same time, we have no clear explanation for the contribution of the single copy-number loss of *PTEN* or *LKB1* or the mutation of *RICTOR* or *PIK3CA* to AST. Nonetheless, our paired sample analysis has unique value because all the post-samples possess an initially identified *EGFR* mutation, which means that the AST is caused by a lineage transition of the existing clone rather than the development of a new primary tumor.

In conclusion, using paired human AST samples, we present positive evidence for the correlation between the PI3K/AKT/mTOR pathway and an ADC to SCC lineage transition that could potentially broaden understanding of the spectrum of mechanisms that lead to *EGFR* TKI resistance in *EGFR*-mutated lung ADC.

Conflict of interest

The authors declare that they have no conflicts of interest.

Funding source

This paper was supported by the following grant(s): The National R & D Program for Cancer Control, Ministry of Health & Welfare, Korea (1720180)

Acknowledgments

None.

Appendix A. Supplementary data

Supplementary material related to this article can be found, in the online version, at doi:https://doi.org/10.1016/j.lungcan.2019.05.024.

References

[1] R. Rosell, E. Carcereny, R. Gervais, A. Vergnenegre, B. Massuti, E. Felip, et al., Erlotinib versus standard chemotherapy as first-line treatment for European patients with advanced EGFR mutation-positive non-small-cell lung cancer (EURTAC): a multicentre, open-label, randomised phase 3 trial, Lancet Oncol. 13 (2012) 239–246.
[2] K. Park, E.H. Tan, K. O'Byrne, L. Zhang, M. Boyer, T. Mok, et al., Afatinib versus gefitinib as first-line treatment of patients with EGFR mutation-positive non-small-cell Lung cancer (LUX-Lung 7): a phase 2B, open-label, randomised controlled trial, Lancet Oncol. 17 (2016) 577–589.
[3] H.A. Yu, M.E. Arcila, N. Rekhtman, C.S. Sima, M.F. Zakowski, W. Pao, et al., Analysis of tumor specimens at the time of acquired resistance to EGFR-TKI therapy in 155 patients with EGFR-mutant lung cancers, Clin. Cancer Res. 19 (2013) 2240–2247.
[4] L.V. Sequist, B.A. Waltman, D. Dias-Santagata, S. Digumarthy, A.B. Turke, P. Fidias, et al., Genotypic and histological evolution of lung cancers acquiring resistance to EGFR inhibitors, Sci. Transl. Med. 3 (2011) 75ra26.
[5] D. Westover, J. Zugazagoitia, B.C. Cho, C.M. Lovly, L. Paz-Ares, Mechanisms of acquired resistance to first- and second-generation EGFR tyrosine kinase inhibitors, Ann. Oncol. 29 (2018) i10–i19.
[6] K.S. Scher, J.S. Saldivar, M. Fishbein, A. Marchevsky, K.L. Reckamp, EGFR-mutated lung cancer with T790M-acquired resistance in the brain and histologic transformation in the lung, J. Natl. Compr. Cancer Netw. 11 (2013) 1040–1044.
[7] J.L. Kuiper, M.I. Ronden, A. Becker, D.A. Heideman, P. van Hengel, B. Ylstra, et al., Transformation to a squamous cell carcinoma phenotype of an EGFR-mutated NSCLC patient after treatment with an EGFR-tyrosine kinase inhibitor, J. Clin. Pathol. 68 (2015) 320–321.
[8] P.A. Levin, M. Mayer, S. Hoskin, J. Sailors, D.H. Oliver, D.E. Gerber, Histologic transformation from adenocarcinoma to squamous cell carcinoma as a mechanism of resistance to EGFR inhibition, J. Thorac. Oncol. 10 (2015) e86–e88.
[9] D.D.G. Bugano, N. Kalhor, J. Zhang, M. Neskey, W.N. William Jr, Squamous-cell transformation in a patient with lung adenocarcinoma receiving erlotinib: co-occurrence with T790M mutation, Cancer Treat. Res. Commun. 4 (2015) 34–36.
[10] L. Longo, M.C. Mengoli, F. Bertolini, S. Bettelli, S. Manfredini, G. Rossi, Synchronous occurrence of squamous-cell carcinoma "transformation" and EGFR exon 20 S768I mutation as a novel mechanism of resistance in EGFR-mutated lung adenocarcinoma, Lung Cancer 103 (2017) 24–26.
[11] E. Roca, M. Pozzari, W. Vermi, V. Tovazzi, A. Baggi, V. Amoroso, et al., Outcome of EGFR-mutated adenocarcinoma NSCLC patients with changed phenotype to squamous cell carcinoma after tyrosine kinase inhibitors: a pooled analysis with an additional case, Lung Cancer 127 (2019) 12–18.
[12] E.L. Jackson, N. Willis, K. Mercer, R.T. Bronson, D. Crowley, R. Montoya, et al., Analysis of lung tumor initiation and progression using conditional expression of oncogenic K-ras, Genes Dev. 15 (2001) 3243–3248.
[13] Z. Chen, C.M. Fillmore, P.S. Hammerman, C.F. Kim, K.K. Wong, Non-small-cell lung cancers: a heterogeneous set of diseases, Nat. Rev. Cancer 14 (2014) 535–546.
[14] A. Jukna, G. Montanari, M.C. Mengoli, A. Cavazza, M. Covi, F. Barbieri, et al., Squamous cell carcinoma "transformation" concurrent with secondary T790M mutation in resistant EGFR-mutated adenocarcinomas, J. Thorac. Oncol. 11 (2016) e49–51.
[15] K. Haratani, H. Hayashi, S. Watanabe, H. Kaneda, T. Yoshida, M. Takeda, et al., Two cases of EGFR mutation-positive lung adenocarcinoma that transformed into squamous cell carcinoma: successful treatment of one case with rociletinib, Ann. Oncol. 27 (2016) 200–202.
[16] H. Izumi, A. Yamasaki, Y. Ueda, T. Sumikawa, H. Maeta, S. Nakamoto, et al., Squamous cell carcinoma transformation from EGFR-mutated lung adenocarcinoma: a case report and literature review, Clin. Lung Cancer 19 (2018) e63–e66.
[17] Cancer Genome Atlas Research Network, Comprehensive genomic characterization of squamous cell lung cancers, Nature 489 (2012) 519–525.
[18] X. Han, F. Li, Z. Fang, Y. Gao, F. Li, R. Fang, et al., Transdifferentiation of lung adenocarcinoma in mice with Lkb1 deficiency to squamous cell carcinoma, Nat. Commun. 5 (2014) 3261.
[19] H. Ji, M.R. Ramsey, D.N. Hayes, C. Fan, K. McNamara, P. Kozlowski, et al., LKB1 modulates lung cancer differentiation and metastasis, Nature 448 (2007) 807–810.
[20] C. Xu, C.M. Fillmore, S. Koyama, H. Wu, Y. Zhao, Z. Chen, et al., Loss of Lkb1 and Pten leads to lung squamous cell carcinoma with elevated PD-L1 expression, Cancer Cell 25 (2014) 590–604.
[21] S. Hou, X. Han, H. Ji, Squamous transition of lung adenocarcinoma and drug resistance, Trends Cancer 2 (2016) 463–466.
[22] H.T. Shin, Y.L. Choi, J.W. Yun, N.K.D. Kim, S.Y. Kim, H.J. Jeon, et al., Prevalence and detection of low-allele-fraction variants in clinical cancer samples, Nat. Commun. 8 (2017) 1377.
[23] C. Lee, J.S. Bae, G.H. Ryu, N.K.D. Kim, D. Park, J. Chung, et al., A method to evaluate the quality of clinical gene-panel sequencing data for single-nucleotide variant detection, J. Mol. Diagn. 19 (2017) 651–658.
[24] H. Li, R. Durbin, Fast and accurate short read alignment with Burrows-Wheeler transform, Bioinformatics 25 (2009) 1754–1760.
[25] A. Wilm, P.P. Aw, D. Bertrand, G.H. Yeo, S.H. Ong, C.H. Wong, et al., LoFreq: a sequence-quality aware, ultra-sensitive variant caller for uncovering cell-population heterogeneity from high-throughput sequencing datasets, Nucleic Acids Res. 40 (2012) 11189–11201.
[26] K. Cibulskis, M.S. Lawrence, S.L. Carter, A. Sivachenko, D. Jaffe, C. Sougnez, et al., Sensitive detection of somatic point mutations in impure and heterogeneous cancer samples, Nat. Biotechnol. 31 (2013) 213–219.

[27] K. Ye, M.H. Schulz, Q. Long, R. Apweiler, Z. Ning, Pindel: a pattern growth approach to detect break points of large deletions and medium sized insertions from paired-end short reads, Bioinformatics 25 (2009) 2865–2871.
[28] S. Lee, J. Seo, J. Park, J.Y. Nam, A. Choi, J.S. Ignatius, et al., Korean Variant Archive (KOVA): a reference database of genetic variations in the Korean population, Sci. Rep. 7 (2017) 4287.
[29] A. Jebali, N. Dumaz, The role of RICTOR downstream of receptor tyrosine kinase in cancers, Mol. Cancer 17 (2018) 39.
[30] M. Riester, A.P. Singh, A.R. Brannon, K. Yu, C.D. Campbell, D.Y. Chiang, et al., PureCN: copy number calling and SNV classification using targeted short read sequencing, Source Code Biol. Med. 11 (2016) 13.
[31] A. Joshi, S. Zanwar, V. Noronha, V.M. Patil, A. Chougule, R. Kumar, et al., EGFR mutation in squamous cell carcinoma of the lung: does it carry the same connotation as in adenocarcinomas? Onco Targets Ther. 10 (2017) 1859–1863.
[32] D.B. Shackelford, R.J. Shaw, The LKB1-AMPK pathway: metabolism and growth control in tumour suppression, Nat. Rev. Cancer 9 (2009) 563–575.
[33] M. Scaltriti, J. Baselga, The epidermal growth factor receptor pathway: a model for targeted therapy, Clin. Cancer Res. 12 (2006) 5268–5272.
[34] M.L. Sos, M. Koker, B.A. Weir, S. Heynck, R. Rabinovsky, T. Zander, et al., PTEN loss contributes to erlotinib resistance in EGFR-mutant lung cancer by activation of Akt and EGFR, Cancer Res. 69 (2009) 3256–3261.